ACS OMEGA

http://pubs.acs.org/journal/acsodf

Article

Miniature β-Hairpin Mimetic by Intramolecular Hydrogen Bond and C−H···π Interactions

Sujay Kumar Nandi, Raju Sarkar, Akhilesh Jaiswar, Susmita Roy,* and Debasish Haldar*

Cite This: *ACS Omega* 2022, 7, 17245−17252

Read Online

ACCESS | Metrics & More | Article Recommendations | Supporting Information

ABSTRACT: Canonically, protein β-hairpin motifs are stabilized by intramolecular hydrogen bonds. Here, we attempt to develop a rational design recipe for a miniature hairpin structure stabilized by hydrogen bonding as well as C−H···π interaction and try to understand how such a stabilization effect varies with different functional groups at each terminus. Database analysis shows that the α-amino acids with an aromatic side chain will not favor that kind of C−H···π stabilized hairpin structure. However, hybrid tripeptides with an N-terminal Boc-Trp-Aib corner residue and C-terminal aromatic ω-amino acids fold into the hairpin conformation with a central β-turn/open-turn that is reinforced by a C−H···π interaction. The CCDC database analysis further confirms that this C−H···π stabilized hairpin motif is general for Boc-protected tripeptides containing Aib in the middle and aromatic functionality at the C-terminus. The different α-amino acids like Leu/Ala/Phe/Pro/Ser at the N-terminus have a minor influence on the C−H···π interaction and stabilities of the folded structures in solid-state. However, the hybrid peptides exhibit different degrees of conformational heterogeneity both in the solid and solution phase, which is common for this kind of flexible small molecule. Conformational heterogeneity in the solution phase including the C−H···π stabilized β-hairpin structures are characterized by the molecular dynamics (MD) simulations explaining their plausible origin at an atomistic level.

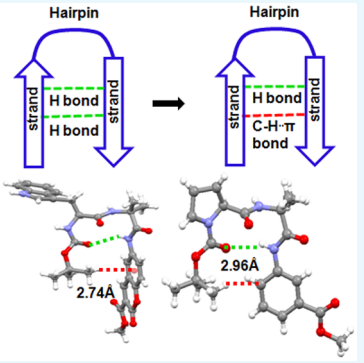

INTRODUCTION

The hairpin structure is one of the major structural motifs found in proteins and peptides.[1−3] The hairpin motif has a crucial role in protein folding.[4] Hairpins are also important as epitopes in protein−protein[5] and protein−nucleic[6] acid interactions.[7] Most hairpins contain a central β-turn.[8] Depending on the dihedral angles φ and ψ of the i + 1 and i + 2 residues, Hutchinson and Thornton defined nine β-turn types such as types I, I′, II, II′, VIa1, VIa2, VIb, VIII, and IV.[9] From the previous report, the β-hairpins of α-peptides have been constructed mostly of the type II′ β-turn of the D-Pro-Gly segment,[10] and the type I′ β- turn of the Asn-Gly[11] and Aib-D-Ala[12] segments of longer peptides. Moreover, the peptides developed from β-, γ-, and ω-amino acids can also form reverse turn structures. Several examples of two-residue hairpin loops consisting of the peptides containing conformationally rigid β-amino acid residues like nipecotic acid or β-2,3-amino acids have formed reverse turns and β-hairpin structures.[13] The effects of conformation are highly important in peptide-based drug design. Peptides with particular conformations have been used as drugs to disrupt protein−protein interactions. The peptide-based natural hormone analogs with distinct conformation have been developed to inhibit intracellular molecules such as receptor tyrosine kinases.[14] Recently, aromatic oligoamide foldamers have been used to mimic the hairpin motif.[15]

The C−H···π interaction is a weak force that arises between CH (soft acids) and π functional groups (soft base).[16] The stability of the C−H···π interaction increases with increasing proton donating ability of the CH groups. The C−H···π interaction takes place in nonpolar as well as polar solvents, even in protic solvents like water. The geometry of C−H···π interactions have wide ranges and the stability depends on the orientation of the C−H and π functionalities.[17] The C−H···π interaction energy is mainly influenced by the arrangement and position of both the CH and π-groups. Previous reports suggested that C−H···π interactions have a key role in the structure and function of proteins including the stabilization of protein structural elements like α-helices, 3_{10} helices, and cis peptide bonds (nonproline).[18−22] Moreover, C−H···π interactions are important for stabilization of particular molecular conformation,[23] chiroptical properties,[24] supramolecular chemistry such as host−guest chemistry,[25] coordination chemistry,[26b] liquid crystals, and clathrates.[26] In biology, thus, C−H···π interactions have been recognized to collectively play a significant role in protein folding, assembly, and biomolecular recognition. In current times, in viral proteins, including in spike proteins, a number of recent investigations found the

Received: February 26, 2022
Accepted: April 28, 2022
Published: May 11, 2022

crucial role of C−H···π interaction in stabilizing protein structure.[27]

Existence of the C−H···π interaction can be proved by different techniques such as the calorimetric method and the comparison of the electronic substituent effect in crystal structure and NMR experiment.[28] The crystallographic database analyses yield strong evidence for C−H···π interaction. Farrugia and co-workers have used both X-ray diffraction and DFT calculations at the B3LYP/6-311++G** level.[28e] However, the experimental investigations of β-hairpin structure of small peptides stabilized by C−H···π interaction are lacking.

Intrigued with that knowledge, in this study we urge to mimic hairpin structure by the folding of short synthetic peptides and understand the effective role of C−H···π interaction in stabilizing the hairpin (Scheme 1). We also

Scheme 1. (A) Hydrogen Bond Stabilized β-Hairpin, (B) C−H···π and Hydrogen Bond Stabilized β-Hairpin, and (c) C−H···π Interaction

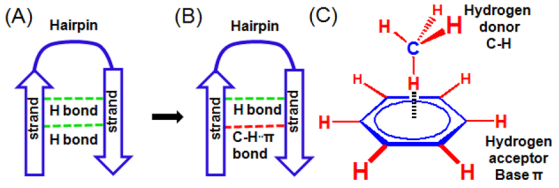

wish to understand the perturbative effects of C-terminal and N-terminal motifs on C−H···π stabilized conformers which may, in turn, exert different degrees of heterogeneity both in the solid and solution phase. To execute this, we plan to replace one of the hydrogen bonds of β-hairpin (Scheme 1A) by C−H···π interaction (Scheme 1B). For C−H···π interaction, the peptide mimetic needs a C−H donor and a hydrogen acceptor π base at the appropriate position (Scheme 1C). For that purpose, we consider having the N-terminal Boc CH as soft acids and C-terminal aromatic amino acid as π functional group (soft base) in a tripeptide.

EXPERIMENTAL SECTION

The reported peptides were synthesized by conventional solution-phase methods using the racemization free fragment condensation strategy. For N-terminal protection, Boc-anhydride was used and the C- terminal was protected as a methyl ester. Couplings were mediated by *N*,*N*′-dicyclohexylcarbodiimide/1-hydroxybenzotriazole (DCC/HOBt). The product was purified by column chromatography using the silica (100−200-mesh size) gel as a stationary phase and *n*-hexane-ethyl acetate mixture as eluent. The final compounds were fully characterized by 400 and 500 MHz ^{1}H NMR spectroscopy, ^{13}C NMR spectroscopy, mass spectrometry, and IR Spectroscopy.

NMR Experiments. All NMR studies were carried out on Brüker Avance 500 MHz and Jeol 400 MHz spectrometers at 298 K. Compound concentrations were in the range 1−10 mM in $CDCl_3$ and DMSO-d_6.

FT−IR Spectroscopy. Solid-state FT−IR spectra were obtained with a PerkinElmer Spectrum RX1 spectrophotometer.

Mass Spectrometry. The mass spectra of the compounds were recorded on a Q-Tof Micro YA263 high-resolution (Waters Corporation) mass spectrometer by electrospray ionization (positive-mode).

Single Crystal X-ray Diffraction Study. Intensity data of all the reported peptides were collected with MoKα radiation using Bruker APEX-2 CCD diffractometer. Data were processed using the Bruker SAINT package and the structure solution and refinement procedures were performed using SHELX97. Single crystal X-ray analysis of tripeptides **1** and **2** were recorded on a Bruker high resolution X-ray diffractometer instruments with MoKα radiation. Data were processed using the Bruker SAINT package and the structure solution and refinement procedures were performed using SHELX97. Crystal data: Tripeptide **1**: $C_{32}H_{36}N_4O_6$, $2(C_2H_6OS)$ M_w = 728.90, *P na* 21, a = 23.8893(6) Å, b = 10.0574(2) Å, c = 30.8929(7) Å, α = 90° β = 90°, γ = 90°, V = 7422.5(3) Å^3, Z = 8, d_m = 1.305 Mg m^{-3}, T = 100 K, $R1$ = 0.0614 and w$R2$ = 0.1565 for 12903 data with $I > 2\sigma(I)$. Tripeptide **2**: $2(C_{31}H_{34}N_4O_8, 2(C_7H_8)$, M_w = 682.76, *P*1, a = 11.4783(2) Å, b = 11.9570(5) Å, c = 15.2501(9) Å, V = 1824.3(2) Å^3, Z = 2, d_m = 1.243 Mg m^{-3}, T = 100, $R1$ = 0.0519 and w$R2$ = 0.1341 for 8780 data with $I > 2\sigma(I)$. CCDC: 2090664 and 2090665 contains the supplementary crystallographic data for foldamer **1** and **2**.

Molecular Dynamics Simulation Details. To study the conformational heterogeneity of peptides 1 and 2, we have performed molecular dynamics (MD) simulations. The initial structural coordinates for all atoms of the peptide molecule were obtained from XRD measurement. All-atom topologies were generated using CHARMM-36 force field and the molecule is cantered in a cubic box having a length of 36.27 Å. The peptide was solvated with a pre-equilibrated TIP3P water model. Since the importance of π-interactions involving aromatic functional groups, such as, CH−π, π−π, lone pair−π, cation−π, and anion−π interactions have been recognized to collectively play a significant role in the folding, assembly, and biomolecular recognition, CHARMM force field and in combination with CHARM-modified TIP3P water model found better in reproducing the preferred binding modes in majority of orientations.[29] In 2005, CHARMM22 first attempted to reproduce the preferred binding modes, with excellent agreement for the benzene dimer. Concurrently, a survey was published focusing on thermodynamic data for the aromatic amino acids and that prompted additional optimization of the tryptophan (Trp) force field.[30] When CHARMM36 force field was developed and the partial charges of Trp ring protons in the CHARMM36 was found better correlated with the observed ring atom participation frequency.[31] Thus, in recent biological studies where the specific participation of CH−π is expected, CHARMM36 and CHARM-modified TIP3P are being used compared to other force fields.[32]

A total of 1551 water molecules were added. In the following steps, energy minimization and equilibration procedures were performed for the system. Energy minimization was done using the steepest descent algorithm and hydrogen bond constraints were added using the LINC algorithm. All the simulations in this study were done at 303.15 K and 1 bar pressure. The temperature was kept constant using the Nose−Hoover thermostat. In the initial equilibration step, the peptide molecule was positionally restrained and an NVT equilibration process has been performed for 0.125 ns. It was followed by an NPT equilibration for 10 ns using the Parinello-Rahman barostat. This MD run was performed removing the position

https://doi.org/10.1021/acsomega.2c01168
ACS Omega 2022, 7, 17245−17252

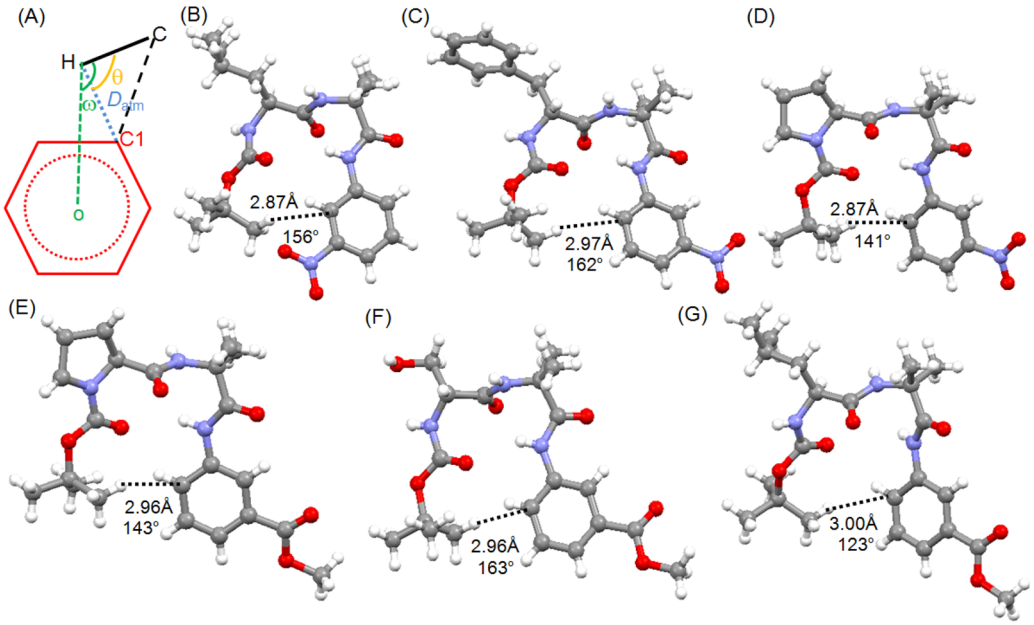

Figure 1. (A) The schematic presentation of surveying C−H···π interaction for a six-member π-system. O: centroid of six-member π-system. D_{atm}: interatomic distance between H and nearest sp^2-carbon. θ: $\angle HCC_{aromatic}$; The solid-state conformations showing C−H···π interactions of (B) Boc-Leu-Aib-*m*-nitroaniline, (C) Boc-Phe-Aib-*m*-nitroaniline, (D) Boc-Pro-Aib-*m*-nitroaniline, (E) Boc-Pro-Aib-Maba-OMe, (F) Boc-Ser-Aib-Maba-OMe, and (G) Boc-Leu-Aib-Maba-Ome.

restraint of the peptide molecule. The final production molecular dynamic simulation was performed for 200 ns at 303.15K. Periodic boundary conditions were applied and nonbonded force calculations employed a grid system for neighbor searching. Neighbor list generation was performed after every 5 steps. A cutoff radius of 1.2 nm was used both for the neighbor list and van der Waal's interaction. To calculate the electrostatic interactions, we used PME with a grid spacing of 0.12 nm and an interpolation order of 4. All the molecular dynamics (MD) simulations have been performed using the GROMACS package.

RESULTS AND DISCUSSION

A database analysis has been performed using the Cambridge Crystallographic Data Centre (CCDC) to understand the role of C−H···π interactions for folding and stability of Boc protected tripeptides containing Aib at the middle and aromatic functionality at the C terminus. C−H···π interactions stabilized turn structures in the CCDC have been identified based purely on geometric criteria. Figure 1A shows the parameters of surveying C−H···π interactions. For C−H···π interactions, the hydrogen atom is positioned above the π plane, considering the charge transfer of the π-electrons to the antibonding orbital of the C−H bond.[33] However, hydrogen does not need to lie exactly above the aromatic system.[34] We have mainly considered the distance of H and aromatic C, D_{atm}, and angle C−H···$C_{aromatic}$ θ (Figure 1A).[16b33] The cutoff for the D_{atm} was 3 Å and for θ was >60°.[37] As shown in Figure 1, couples of tripeptides having Boc protection at N-terminus and an aromatic moiety at C-terminal has shown C−H···π interactions in solid-state. Boc-Leu-Aib-*m*-nitroaniline[35] (Figure 1B) and Boc-Phe-Aib-*m*-nitroaniline[35] (Figure 1C) exhibit C−H···π interactions due to charge transfer of the π-electrons to the antibonding orbital of the C−H bond. Replacing Leu with Ser residue and *m*-aminobenzoic acid has a minor influence on the C−H···π interaction and stabilities of the folded structures (Figure 1F, Boc-Ser-Aib-Maba-OMe[36] and Figure 1G, Boc-Leu-Aib-Maba-OMe).[36] Even incorporation of proline has an insignificant effect on the C−H···π stabilized hairpin conformation (Figure 1D, Boc-Pro-Aib-*m*-nitroaniline and Figure 1E, Boc-Pro-Aib-Maba-OMe).[37] So, on the basis of the crystal structures of compounds **1** and **2**, we confirm the C−H···π interaction and formation of C−H···π interaction stabilized β-hairpin structure. The C-terminal aromatic units with different properties (electron-rich or poor) have a minor influence on the C−H···π interaction and stabilities of the folded structures. As we need a CH that can act as soft acids for C−H···π interaction, we cannot use other N-terminal protecting groups like trityl (trt), 3,5-dimethoxyphenylisopropoxycarbonyl (Ddz), 2-(4-biphenyl)isopropoxycarbonyl (Bpoc), 2-nitrophenylsulfenyl (Nps), 9-fluorenylmethoxycarbonyl (Fmoc), 2-(4-nitrophenylsulfonyl)ethoxycarbonyl (Nsc), 1,1-dioxobenzo[b]thiophene-2- ylmethyloxycarbonyl (Bsmoc), tetrachlorophthaloyl (TCP), 2-chlorobenzyloxycarbonyl (Cl-Z), and benzyloxycarbonyl (Z) for control experiments.

So, in peptide design, at C-terminus, instead of α-amino acids with aromatic side chain, we have incorporated β/ω-amino acid with an aromatic backbone (Scheme 2). From Scheme 2, the tripeptide can fold into a hydrogen-bonded β-turn structure and the N-terminal Boc CH can act as a soft acid and C-terminal aromatic amino acid as π functional group (soft

Scheme 2. Diagram of Hybrid Tripeptide Folds into a C−H···π and Hydrogen-Bond Stabilized β-Hairpin Structure

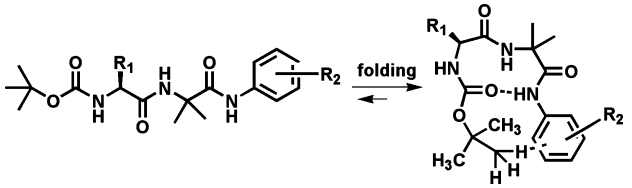

https://doi.org/10.1021/acsomega.2c01168
ACS Omega 2022, 7, 17245−17252

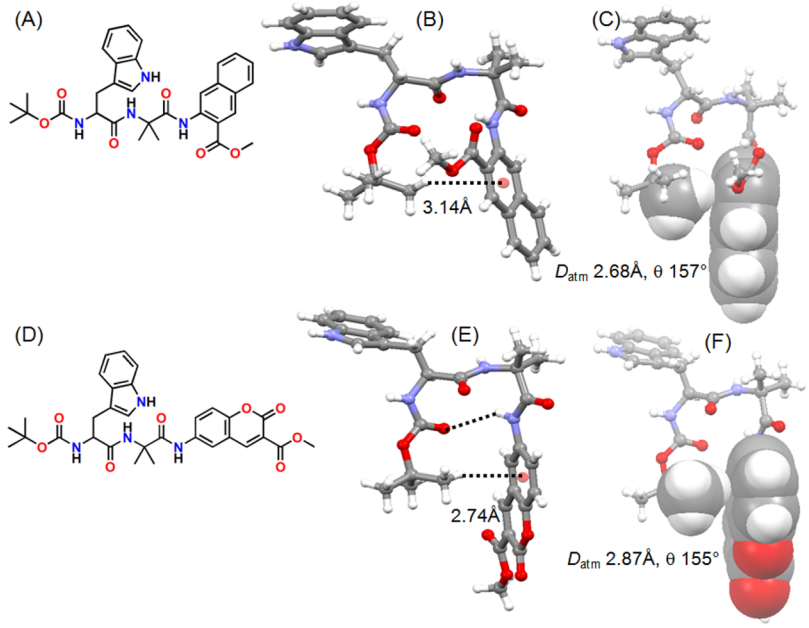

Figure 2. (A) The schematic presentation of peptide **1**; (B) solid-state conformation of peptide **1A** showing C−H···π interactions; (C) space fill model of peptide **1A** showing C−H···π interactions and parameters; (D) schematic presentation of peptide **2**, (E) solid-state conformation of peptide **2A** showing hydrogen bonding and C−H···π interactions; and (F) space fill model of peptide **2A** showing C−H···π interactions and parameters.

Table 1. Selected Backbone Torsion Angles (deg) for Peptides 1 and 2

	φ_1 (deg)	ψ_1 (deg)	φ_2 (deg)	ψ_2 (deg)	φ_3 (deg)	ψ_3 (deg)
Peptide **1A**	59.54	−143.06	−52.94	−41.49	172.88	156.24
Peptide **1B**	−61.48	143.49	51.74	42.90	−170.33	−154.42
Peptide **2A**	44.87	−131.29	−59.26	−29.61	153.57	−169.39
Peptide **2B**	−53.05	149.64	57.52	32.24	−163.80	173.26

base) and show C−H···π interaction. Thus, a miniature β-hairpin structure stabilized by intramolecular hydrogen bond and C−H···π interaction may appear.

From our previous report, we learn that Boc-Trp-Aib can act as a corner residue for β-turn mimetic.[38] For foldamers **1** and **2** (Figure 2a,d), we have incorporated Boc-Trp-Aib as a corner residue and 3-amino-naphthalene-2-carboxylic acid and 6-amino-coumarin-3-carboxylic acid as π functional group (soft base) at the C-terminus. The design principle was, the Boc-Trp-Aib as a corner residue will help to form an intramolecular hydrogen-bonded β-turn structure, like many other reported Aib containing tripeptides.[39] The C-terminal aromatic moiety may help to stabilize the motif with additional C−H···π interactions with Boc CH. Target tripeptides **1** and **2** were synthesized by conventional solution-phase methodology following a high purity, as confirmed by ^{1}H NMR, ^{13}C NMR, FT−IR spectroscopy, and mass spectrometry (MS) analysis (see Supporting Information, SI).

Solid-state FT−IR spectroscopy is a reliable technique to study the conformational preferences of the foldamers. The FT−IR spectrum of foldamer **1** (SI Figure S1a) exhibits an intense band at 3295 cm^{-1} indicative of the presence of hydrogen-bonded NH groups. The amide I bands at 1663, 1650 cm^{-1}, and amide II band at 1507 cm^{-1} suggest that the foldamer **1** adopts a hydrogen-bonded turn-like structure.[40] For foldamer **2**, a band at 3253 cm^{-1} indicates the presence of hydrogen-bonded NH groups. The amide I band at 1658 cm^{-1} and amide II bands at 1514, 1502 cm^{-1} (SI Figure S1b) suggests a similar turn structure for foldamer **2**.[40]

Single crystal X-ray analysis sheds some light on the molecular conformation of the tripeptides. Colorless crystals of tripeptides **1** and **2** were obtained from DMSO and toluene solutions respectively by slow evaporation. From X-ray crystallography, the asymmetric unit contains two molecules of peptide **1** (termed as **1A** and **1B**) and four molecules of DMSO (SI Figure S2). Two DMSO molecules are hydrogen-bonded with the indole NH of tryptophan and the rest DMSO units are hydrogen-bonded with the Aib NH's. The ORTEP diagram (SI Figure S2) of peptide **1** shows that the peptide **1A** backbone adopts a distorted type II′ β-turn conformation and peptide **1B** backbone has a distorted type II β-turn conformation, though there is no 10-member intramolecular N−H···O hydrogen bond. The important backbone torsion angles are listed in Table 1. In the asymmetric unit, the peptide **1** molecules (A and B) are in an antiparallel position and linked by two intermolecular hydrogen bonds between reciprocal Trp NH and Trp C═O functional groups. The overlay of peptides **1A** and **1B** show a significant difference in the position of peptides bonds and aromatic and hydrophobic side chains (SI Figure S3). The folded structure of the peptide **1A** molecule is further stabilized by a C−H···π interaction between Boc CH and C-terminal aromatic β-amino acid (D_{atm} 2.68 Å, θ 157°, C−H to centroid distance 3.14 Å) (Figure 2B,C). The peptide **1B** molecule is also stabilized by a C−H···π interaction between Boc CH and the C-terminal

https://doi.org/10.1021/acsomega.2c01168
ACS Omega 2022, 7, 17245−17252

aromatic β-amino acid (D_{atm} 2.72 Å, θ 155°, C−H to centroid distance 3.19 Å) (SI Figure S4). Two molecules of peptide **2** crystallize with two molecules of toluene in the asymmetric unit (SI Figure S5). Two toluene molecules are accompanied by peptide **2** molecules through strong face-to-face $\pi-\pi$ stacking interactions with the coumarin functionality (centroid to centroid distance 3.54 Å) (SI Figure S6). The torsion angle around the conformationally constrained Aib residues (−59.26° and −29.61°) plays a crucial role in dictating the distorted type II′ β-turn-like conformation of **2A**. The backbone torsion angles of peptide **2** are listed in Table 1. There is an intramolecular 10-member N−H···O hydrogen bond between the Boc C═O and NH of the 6-amino-coumarin-3-carboxylic acid (Figure 2E). The folded structure of the peptide **2A** molecule is further stabilized by a C−H···π interaction between the Boc CH and 6-amino-coumarin-3-carboxylic acid (D_{atm} 2.83 Å, θ 155°, C−H to centroid distance 2.74 Å) (Figure 2E,F). The peptide **2B** molecule with an open turn structure is also stabilized by a C−H···π interaction between Boc CH and C-terminal 6-amino-coumarin-3-carboxylic acid (D_{atm} 2.95 Å, θ 162°, C−H to centroid distance 2.84 Å). The overlay of **2A** and **2B** show significant heterogeneity in backbone conformation (SI Figure S7). In higher-order packing, the peptide **1** molecules are themselves regularly interlinked through multiple $\pi-\pi$ stacking interactions and thereby form a supramolecular cage-like structure along the crystallographic *a* and *c* direction (SI Figure S8). However, in packing, peptide **2** molecules form a sheet-like structure (SI Figure S9). The hydrogen bonding parameters of **1** and **2** are listed in Table S1.

To study the conformational preferences of the foldamers **1** and **2** in solution, solvent titration experiments have been performed. The effects of adding a hydrogen bond accepting solvent like $(CD_3)_2SO$ to $CDCl_3$ solutions of peptides **1** and **2** are presented in Figure 3A. Generally, the addition of small amounts of $(CD_3)_2SO$ to $CDCl_3$ brings about monotonic downfield shifts of exposed NH groups in peptides, leaving solvent-shielded NH groups largely unaffected.[41] Figure 3A shows that for both peptides **1** and **2**, Boc and Aib NHs are solvent-exposed. For both peptides, residue **3** NH exhibits minimum chemical shift ($\Delta\delta$ 0.02 for peptide **1** and 0.05 for peptide **2**) even at higher percentages of $(CD_3)_2SO$. However, the Aib NH shows a maximum chemical shift ($\Delta\delta$ 0.80 for peptide **1** and 0.43 for peptide **2**). SI Table S2 illustrates $\Delta\delta$ values of all amide NHs for peptides **1** and **2**. This demonstrates that peptides **1** and **2** form intramolecular hydrogen-bonded structures in solution.[42] While the effects of varying concentration, temperature, and solvent polarity on the H-bonding interactions involving protons of peptides **1** and **2** point to the adoption of the β-turn conformation, the folded structures of these hybrid peptides were studied by 2D NMR spectra recorded in $CDCl_3$ solution. The NOESY spectrum exhibits NOE intensities which are responsible for intramolecular interaction between Boc protons with aromatic protons and methyl ester protons of peptide **1** (Figures 3B and S10). For peptide **2** also, the NOESY spectrum exhibits NOE intensities which are responsible for the intramolecular interaction between Boc protons with aromatic protons only, as the methyl ester protons are at the far end of the aromatic ring (Figures 3C and S11). From the NOESY spectrum, the NOEs observed with foldamers **1** and **2** (Figure 3B,C, red arrows) share a general pattern that is responsible for a β-hairpin conformation where two termini of each hybrid

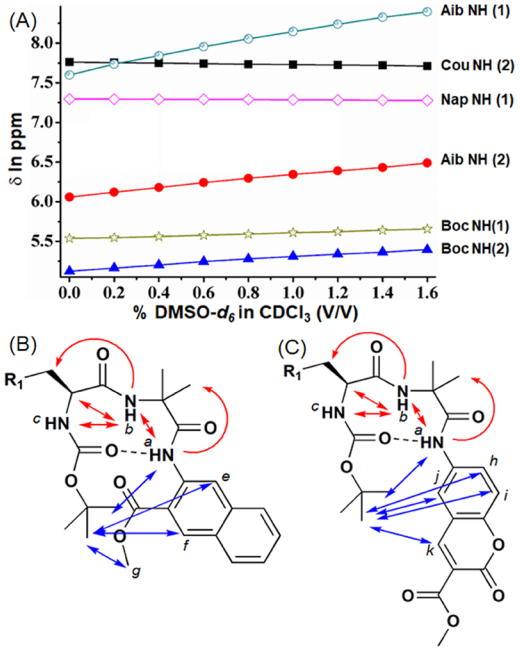

Figure 3. (A) Plot of solvent dependence of NH chemical shifts for peptides **1** and **2** at varying concentrations of $(CD_3)_2SO$ in $CDCl_3$ solutions. The indole NH of Trp side chains have not been included; NOEs (shown as blue and red arrows) between remote (non-adjacent) protons revealed by the NOESY spectra in $CDCl_3$ (5 mM, 298 K, 500 MHz) of (B) peptide **1** and (C) peptide **2**.

peptide are brought into close proximity in the folded conformation. These multiple NOEs confirm that despite their different α- and ω-amino acid residues, the hybrid peptides all fold into similar hairpin conformations, albeit with different stabilities. Moreover, the NOESY spectrum also indicates the presence of other conformations of peptides **1** and **2** in solution. This kind of conformational heterogeneity of flexible small peptides in solution is quite common. The solid-state structure may be considered to be a snapshot of one of the many possible conformations of the small peptides.

Further, to study the conformational heterogeneity and plasticity of peptides **1** and **2**, we have combined 2D NOESY spectra and Atomistic Molecular Dynamics (MD) simulations to determine their three-dimensional conformational states in solution. The MD simulation has been performed using the CHARMM-36 force field[43,44] and TIP3P[45] water model to obtain the equilibrium conformational states of the peptides (the simulation method details are described in the SI and equilibration is verified in SI Figures S12 and S13).[45] However, in different MD studies specific C−H···π interactions are well validated with the combination of CHARMM-36 and modified CHARMM-36(CHARMM-36m) compared to other biomolecular force-fields. To define the conformational heterogeneity of peptide **1** we have defined dihedral angles, φ and ψ, around the central Aib residue (Figure 4A). Figure 4B shows the four distinct structural ensembles of peptide **1** in conformational space of φ and ψ. The emergence of two rotamers, state A and state C, indeed reflects the stabilization of C−H···π induced hairpin fold. However, due to the subtle interference of an adjacent *t*-butyl segment of 3-amino-naphthalene-2-carboxylic acid, a highly dynamic folding behavior is observed resulting in two other states D and E for peptide **1**, in solution. Although the degree of conformational heterogeneity reflected by the

https://doi.org/10.1021/acsomega.2c01168
ACS Omega 2022, 7, 17245−17252

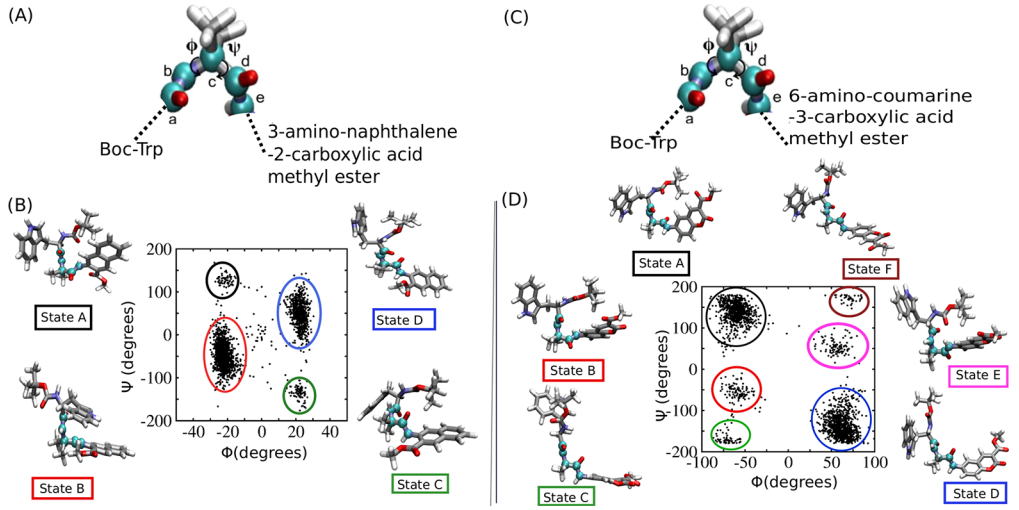

Figure 4. (A) Defining backbone PHI(Φ), PSI(Ψ) dihedral angles around Aib residue of peptide 1. (B) Conformational phase-space as a function of PHI, PSI dihedrals calculated from atomistic MD simulation trajectories extracted by simulating the peptide 1. (C) Defining backbone PHI(Φ), PSI(Ψ) dihedral angles around Aib residue of peptide 2. (D) Conformational phase-space as a function of PHI, PSI dihedral angles calculated from atomistic MD simulation trajectories extracted by simulating the peptide **2** in water.

torsion angles measurement (Table 1 and Figure 4) in the solid and solution phase would appear differently, the population of C−H···π stabilized β-hairpin conformations still emerge both in solid and solution phase. The emergence of C−H···π stabilized conformations are compared in both the solid and solution phase based on the geometric criteria as defined in Figure 4A. As for peptide **1**, C−H···π stabilization in state A occurs through $D_{atm} \approx 2.90$ Å, $\theta \approx 110.84°$ and for state C, they are $D_{atm} \approx 2.77$ Å, $\theta \approx 123.89°$ which is comparable with the experimental findings. Similarly, for peptide **2**, we have defined dihedral angles, φ and ψ, around the central Aib residue (Figure 4C). In comparison to peptide **1**, the distant spatial allocation of the *t*-butyl segment in 6-amino-coumarin-3-carboxylic acid at the C-terminus and its lower interference helps peptide **2** to mostly stay in its folding states as depicted in Figure 4D. For peptide **2**, we obtain four (out of a total of six conformations) diverse, highly populated ensembles that are indeed C−H···π induced folded hairpin structures (state A, B, E). Among them, state E represents a rich β-hairpin conformation stabilized by both the N−H···O hydrogen bond between Boc C═O and NH of 6-amino-coumarin-3-carboxylic acid and C−H···π interactions. Besides, time-dependent fluctuations of two dihedral angles entail that the ψ angle is more sensitive to molecular modification than φ for both peptides (SI Figures S14−S16). This signifies that these hybrid tripeptides have the potential to show more sensitivity to changes made over the C-terminus. Here, for peptide **2**, C−H···π stabilization in state A occurs through $D_{atm} \sim 2.90$ Å, $\theta \sim 135.40°$ and for state B, they are $D_{atm} \sim 3.01$ Å, $\theta \sim 126.42°$, and for state E, they are $D_{atm} \sim 2.82$ Å, $\theta \sim 152.19°$, which is correlating with the solid-state folded structure of peptide **2A** molecule shown in Figure 2F.

Further, we have performed a database analysis (Cambridge Crystallographic Data Centre, CCDC) for the crystal structures of tripeptides with a Boc protecting group at the N-terminus, α-aminoisobutyric acid (Aib) at the middle, and α-amino acids with an aromatic side chain (Phe/Tyr/Trp) at C-terminus. Aib is helicogenic and will be helpful for reverse turn formation. For the C−H···π interaction, the selected C−H···C distance was 3 Å. However, the analysis shows that the tripeptides containing C-terminal α-amino acids with aromatic side chain did not favored that kind of C−H···π interactions with Boc CH. The tripeptides Boc-Leu-Aib-Tyr-OMe, Boc-Leu-Aib-Phe-OMe,[46] Boc-Ile-Aib-Phe-OMe,[47] Boc-Ser-Aib-Tyr-OMe,[48] Boc-Phe-Aib-Phe-OMe,[49] and Boc-Ile-Aib-Tyr-OMe[48] adopt different conformations, and there is no C−H···π interaction between Boc CH and aromatic functionalities.

CONCLUSIONS

In conclusion, we have shown that the hybrid tripeptides, having a common backbone with an N-terminal Boc-Trp-Aib corner residue and a C-terminal aromatic ω-amino acids fold into the hairpin conformation with a central β-turn/open-turn that is reinforced by a C−H···π interaction. This hairpin motif is general and can accommodate different α-amino acids at the N-terminus and aromatic ω-amino acids at the C-terminus. This hypothesis is further supported by the CCDC database analysis. The hybrid peptides show different degrees of conformational heterogeneity in the solid and solution phases. The conformational heterogeneity, including the C−H···π stabilized β-hairpin structures, were further characterized by the MD simulations. Nonetheless, our dihedral angle calculations around the peptide backbone and their time-dependent fluctuations show a more dynamic response originating from the C-terminus rather than the Boc-protected N-terminus. This provides an atomistic-level of understanding and also a plausible explanation behind the lower sensitivity of the N-terminus toward molecular modification. The results presented here may foster new studies to rationally mimic the biological motif and their function following an in-depth understanding-based approach.

ASSOCIATED CONTENT

Supporting Information

The Supporting Information is available free of charge at https://pubs.acs.org/doi/10.1021/acsomega.2c01168.

Synthesis and characterization of compounds, ^{1}H NMR, ^{13}C NMR, solid-state FTIR spectra, MD method, Figures SI S1−15, Figures S16−S33; CCDC 2090664 and 2090665 (PDF)

https://doi.org/10.1021/acsomega.2c01168
ACS Omega 2022, 7, 17245−17252

AUTHOR INFORMATION

Corresponding Authors

Debasish Haldar − *Department of Chemical Sciences, Indian Institute of Science Education and Research Kolkata, Nadia, West Bengal 741246, India;* orcid.org/0000-0002-7983-4272; Email: deba_h76@yahoo.com, deba_h76@iiserkol.ac.in

Susmita Roy − *Department of Chemical Sciences, Indian Institute of Science Education and Research Kolkata, Nadia, West Bengal 741246, India;* orcid.org/0000-0001-6411-4347; Email: susmita.roy@iiserkol.ac.in

Authors

Sujay Kumar Nandi − *Department of Chemical Sciences, Indian Institute of Science Education and Research Kolkata, Nadia, West Bengal 741246, India*

Raju Sarkar − *Department of Chemical Sciences, Indian Institute of Science Education and Research Kolkata, Nadia, West Bengal 741246, India*

Akhilesh Jaiswar − *Department of Chemical Sciences, Indian Institute of Science Education and Research Kolkata, Nadia, West Bengal 741246, India*

Complete contact information is available at: https://pubs.acs.org/10.1021/acsomega.2c01168

Author Contributions

S.K.N. has synthesized and analyzed the compounds. R.S. and S.J. have performed the computational works. S.R. and D.H. performed the analysis and wrote the manuscript.

Notes

The authors declare no competing financial interest.

ACKNOWLEDGMENTS

S.K.N. acknowledges the CSIR, India and A.J. acknowledges the UGC for the research fellowship. We thank IISER-Kolkata for the instrumental facility. A.J. and S.R. thank the DIRAC supercomputing facility, IISER-Kolkata. S.R. acknowledges support from DBT, India (Grant No. BT/12/IYBA/2019/12) and SERB, DST, Govt. of India (Grant No. SRG/2020/001295).

REFERENCES

(1) (a) Ke, P. C.; Zhou, R.; Serpell, L. C.; Riek, R.; Knowles, T. P. J.; Lashuel, H. A.; Gazit, E.; Hamley, I. W.; Davis, T. P.; Fändrich, M.; Otzen, D. E.; Chapman, M. R.; Dobson, C. M.; Eisenberg, D. S.; Mezzenga, R. Half a century of amyloids: past, present and future. *Chem. Soc. Rev.* **2020**, *49*, 5473−5509. (b) Richardson, J. S. The Anatomy and Taxonomy of Protein Structure. *Adv. Protein Chem.* **1981**, *34*, 167−339. (c) Nair, R. V.; Kotmale, A. S.; Dhokale, S. A.; Gawade, R. L.; Puranik, V. G.; Rajamohanan, P. R.; Sanjayan, G. J. Formation of a pseudo-β-hairpin motif utilizing the Ant−Pro reverse turn: consequences of stereochemical reordering. *Org. Biomol. Chem.* **2014**, *12*, 774−782. (d) Abhishek, S.; Deeksha, W.; Rajakumara, E. Helical and β-Turn Conformations in the Peptide Recognition Regions of the VIM1 PHD Finger Abrogate H3K4 Peptide Recognition. *Biochemistry* **2021**, *60* (35), 2652−2662.

(2) (a) Das, C.; Raghothama, S.; Balaram, P. A Designed Three Stranded β-Sheet Peptide as a Multiple β-Hairpin Model. *J. Am. Chem. Soc.* **1998**, *120*, 5812−5813. (b) Karle, I.; Gopi, H. N.; Balaram, P. Infinite pleated β-sheet formed by the β-hairpin Boc-β-Phe-β-Phe-D-Pro-Gly-β-Phe-β-Phe-OMe. *Proc. Natl. Acad. Sci. U.S.A.* **2002**, *99*, 5160−5164.

(3) Dinner, A. R.; Lazaridis, T.; Karplus, M. Understanding β-hairpin formation. *Proc. Natl. Acad. Sci. U.S.A.* **1999**, *96*, 9068−9073.

(4) (a) Lahiri, P.; Verma, H.; Ravikumar, A.; Chatterjee, J. Protein stabilization by tuning the steric restraint at the reverse turn. *Chem. Sci.* **2018**, *9*, 4600−4609. (b) Kobayashi, N.; Honda, S.; Yoshii, H.; Munekata, E. Role of Side-chains in the Cooperative β-Hairpin Folding of the Short C-Terminal Fragment Derived from Streptococcal Protein G. *Biochemistry* **2000**, *39*, 6564−6571. (c) Oddo, A.; Mortensen, S.; Thøgersen, H.; De Maria, L.; Hennen, S.; McGuire, J. N.; Kofoed, J.; Linderoth, L.; Reedtz-Runge, S. α-Helix or β-Turn? An Investigation into N-Terminally Constrained Analogues of Glucagon-like Peptide 1 (GLP-1) and Exendin-4. *Biochemistry* **2018**, *57*, 4148−4154.

(5) Tyndall, J. D. A.; Pfeiffer, B.; Abbenante, G.; Fairlie, D. P. Over One Hundred Peptide-Activated G Protein-Coupled Receptors Recognize Ligands with Turn Structure. *Chem. Rev.* **2005**, *105*, 793−826.

(6) Shi, Y.; Wang, Y. F.; Jayaraman, L.; Yang, H.; Massague, J.; Pavletich, N. P. Crystal Structure of a Smad MH1 Domain Bound to DNA: Insights on DNA Binding in TGF-β Signaling. *Cell* **1998**, *94*, 585−594.

(7) (a) Venkatraman, J.; Shankaramma, S. C.; Balaram, P. Design of Folded Peptides. *Chem. Rev.* **2001**, *101*, 3131−3152. (b) Aemissegger, A.; Krautler, V.; van Gunsteren, W. F.; Hilvert, D. A Photoinducible β-Hairpin. *J. Am. Chem. Soc.* **2005**, *127*, 2929−2936.

(8) Vass, E.; Hollósi, M.; Besson, F.; Buchet, R. Vibrational Spectroscopic Detection of Beta- and Gamma-Turns in Synthetic and Natural Peptides and Proteins. *Chem. Rev.* **2003**, *103*, 1917−1954.

(9) Hutchinson, E. G.; Thornton, J. M. A revised set of potentials for β-turn formation in proteins. *Protein Sci.* **1994**, *3*, 2207−2216.

(10) Syud, F. A.; Stanger, H. E.; Gellman, S. H. Interstrand Side Chain-Side Chain Interactions in a Designed β-Hairpin: Significance of Both Lateral and Diagonal Pairings. *J. Am. Chem. Soc.* **2001**, *123*, 8667−8677.

(11) Simpson, E. R.; Meldrum, J. K.; Bofill, R.; Crespo, M. D.; Holmes, E.; Searle, M. S. Engineering Enhanced Protein Stability through β-Turn Optimization: Insights for the Design of Stable Peptide β-Hairpin Systems. *Angew. Chem., Int. Ed.* **2005**, *44*, 4939−4944.

(12) Aravinda, S.; Shamala, N.; Rajkishore, R.; Gopi, H. N.; Balaram, P. A Crystalline β-Hairpin Peptide Nucleated by a Type I′ Aib-D-Ala β-Turn: Evidence for Cross-Strand Aromatic Interactions. *Angew. Chem., Int. Ed.* **2002**, *41*, 3863−3865.

(13) (a) Chung, Y. J.; Huck, B. R.; Christianson, L. A.; Stanger, H. E.; Krauthäuser, S.; Powell, D. R.; Gellman, S. H. Stereochemical Control of Hairpin Formation in β-Peptides Containing Dinipecotic Acid Reverse Turn Segments. *J. Am. Chem. Soc.* **2000**, *122*, 3995−4004. (b) Daura, X.; Gademann, K.; Schäfer, H.; Jaun, B.; Seebach, D.; van Gunsteren, W. F. The β-Peptide Hairpin in Solution: Conformational Study of a β-Hexapeptide in Methanol by NMR Spectroscopy and MD Simulation. *J. Am. Chem. Soc.* **2001**, *123*, 2393−2404.

(14) Chang, Y. S.; Graves, B.; Guerlavais, V.; Tovar, C.; Packman, K.; To, K.-H.; Olson, K. A.; Kesavan, K.; Gangurde, P.; Mukherjee, A.; Baker, T.; Darlak, K.; Elkin, C.; Filipovic, Z.; Qureshi, F. Z.; Cai, H.; Berry, P.; Feyfant, E.; Shi, X. E.; Horstick, J.; Annis, D. A.; Manning, A. M.; Fotouhi, N.; Nash, H.; Vassilev, L. T.; Sawyer, T. K.; et al. Stapled alpha-helical peptide drug development: A potent dual inhibitor of MDM2 and MDMX for p53-dependent cancer therapy. *Proc. Natl. Acad. Sci. U.S.A.* **2013**, *110*, 3445−3454.

(15) (a) Tang, Q.; Zhong, Y.; Miller, D. P.; Liu, R.; Zurek, E.; Lu, Z.-L.; Gong, B. Reverse Turn Foldamers: An Expanded β□Turn Motif Reinforced by Double Hydrogen Bonds. *Org. Lett.* **2020**, *22*, 1003−1007. (b) Sebaoun, L.; Maurizot, V.; Granier, T.; Kauffmann, B.; Huc, I. Aromatic Oligoamide β□Sheet Foldamers. *J. Am. Chem. Soc.* **2014**, *136*, 2168−2174.

(16) (a) Nishio, M.; Hirota, M. CH/π interaction: Implications in organic chemistry. *Tetrahedron* **1989**, *45*, 7201−7245. (b) Nishio, M. The CH/π hydrogen bond in chemistry. Conformation, supramolecules, optical resolution and interactions involving carbohydrates. *Phys. Chem. Chem. Phys.* **2011**, *13*, 13873−13900.

(17) Nishio, M.; Hirota, M.; Umezawa, Y. *The CH/π Interaction. Evidence, Nature and Consequences*; John Wiley and Sons, Inc.: New York, 1998.
(18) Brandl, M.; Weiss, M. S.; Jabs, A.; Sühnel, J.; Hilgenfeld, R. C-H···π-interactions in proteins. *J. Mol. Biol.* **2001**, *307*, 357−377.
(19) Baker, E. G.; Williams, C.; Hudson, K. L.; Bartlett, G. J.; Heal, J. W.; Goff, K. L P.; Sessions, R. B.; Crump, M. P.; Woolfson, D. N. Engineering protein stability with atomic precision in a monomeric miniprotein. *Nat. Chem. Biol.* **2017**, *13*, 764−770.
(20) Ganguly, H. K.; Kaur, H.; Basu, G. Local control of cis-peptidyl-prolyl bonds mediated by CH···π interactions: the Xaa-Pro-Tyr motif. *Biochemistry* **2013**, *52*, 6348−6357.
(21) Ghosh, P.; Chatterjee, J. CH−π interaction between cross-strand amino acid pairs stabilizes β-hairpins. *Chem. Commun.* **2020**, *56*, 14447−14450.
(22) Zondlo, N. J. Aromatic−Proline Interactions: Electronically Tunable CH/π Interactions. *Acc. Chem. Res.* **2013**, *46*, 1039−1049.
(23) Shimizu, H.; Yonezawa, T.; Watanabe, T.; Kobayashi, K. Novel cycloaddition of 2-alkyl-3-benzoyl-2-thianaphthales. *Chem. Commun.* **1996**, 1659−1660.
(24) Araki, S.; Seki, T.; Sakakibara, K.; Hirota, M.; Kodama, Y.; Nishio, M. Effect of CH/π interaction on the chiroptical properties of olefins and dienes. *Tetrahedron: Asymmetry* **1993**, *4*, 555−574.
(25) Imai, H.; Uemori, Y. Effects of organization of zinc porphyrin hosts on binding enhancements and recognition of axial ligands. *J. Chem. Soc. Perkin Trans. 2* **1994**, 1793−1797.
(26) (a) Mori, A.; Hirayama, K.; Kato, N.; Takeshita, H.; Ujiie, S. New Troponoid Liquid Crystalline Compounds, 5-Alkoxy-2-(4-alkoxybenzoylamino)tropones. *Chem. Lett.* **1997**, *26*, 509−510. (b) Klarner, F.-G.; Benkhoff, J.; Boese, R.; Burkert, U.; Kamieth, M.; Naatz, U. Molecular Tweezers as Synthetic Receptors in Host-Guest Chemistry: Inclusion of Cyclohexane and Self-Assembly of Aliphatic Side Chains. *Angew. Chem., Int. Ed. Engl.* **1996**, *35*, 1130−1133.
(27) (a) Roy, S.; Jaiswar, A.; Sarkar, R. Dynamic Asymmetry Exposes 2019-nCoV Prefusion Spike. *J. Phys. Chem. Lett.* **2020**, *11*, 7021−7027. (b) Fantini, J.; Di Scala, C.; Chahinian, H.; Yahi, N. Structural and molecular modelling studies reveal a new mechanism of action of chloroquine and hydroxychloroquine against SARS-CoV-2 infection. *Int. J. Antimicrob. Agents* **2020**, *55*, 105960.
(28) (a) Miyake, H.; Kamon, H.; Miyahara, I.; Sugimoto, H.; Tsukube, H. Time-Programmed Peptide Helix Inversion of a Synthetic Metal Complex Triggered by an Achiral NO_3^- Anion. *J. Am. Chem. Soc.* **2008**, *130*, 792−793. (b) Karim, A. R.; Linden, A.; Baldridge, K. K.; Siegel, J. S. Symmetry and polar-π effects on the dynamics of enshrouded aryl-alkyne molecular rotors. *Chem. Sci.* **2010**, *1*, 102−110. (c) Dikundwar, A. G.; Venkateswarlu, C.; Piltz, R. O.; Chandrasekaran, S.; Guru Row, T. N. Crystal structures of fluorinated aryl biscarbonates and a biscarbamate: a counterpoise between weak intermolecular interactions and molecular symmetry. *CrystEngComm* **2011**, *13*, 1531−1538. (d) Katrusiak, A.; Podsiadło, M.; Budzianowski, A. Association CH···π and No van der Waals Contacts at the Lowest Limits of Crystalline Benzene I and II Stability Regions. *Cryst. Growth Des.* **2010**, *10*, 3461−3465. (e) Farrugia, L. J.; Kocovsky, P.; Senn, H. M.; Vyskocil, S. Weak intra- and intermolecular interactions in a binaphthol imine: an experimental charge-density study on (±)-8′-benzhydrylideneamino-1,1′-binaphthyl-2-ol. *Acta Crystallogr., Sect. B: Struct. Sci.* **2009**, *65*, 757−769.
(29) Chakravarty, S.; Ung, A. R.; Moore, B.; Shore, J.; Alshamrani, M. A Comprehensive Analysis of Anion−Quadrupole Interactions in Protein Structures. *Biochemistry* **2018**, *57*, 1852−1867.
(30) Macias, A. T.; Mackerell, A. D. J. CH/Pi Interactions Involving Aromatic Amino Acids: Refinement of the CHARMM Tryptophan Force Field. *J. Comput. Chem.* **2005**, *26*, 1452−1463.
(31) Khan, H. M.; MacKerell, A. D.; Reuter, N. Cation-π Interactions between Methylated Ammonium Groups and Tryptophan in the CHARMM36 Additive Force Field. *J. Chem. Theory Comput.* **2019**, *15*, 7−12.
(32) Fantini, J.; Di Scala, C.; Chahinian, H.; Yahi, N. Structural and Molecular Modelling Studies Reveal a New Mechanism of Action of Chloroquine and Hydroxychloroquine against SARS-CoV-2 Infection. *Int. J. Antimicrob. Agents* **2020**, *55*, 105960.
(33) Umezawa, Y.; Tsuboyama, S.; Honda, K.; Uzawa, J.; Nishio, M. CH/π Interaction in the Crystal Structure of Organic Compounds. A Database Study. *Bull. Chem. Soc. Jpn.* **1998**, *71*, 1207−1213.
(34) Wang, J.; Yao, L. Dissecting C−H···π and N−H···π Interactions in Two Proteins Using a Combined Experimental and Computational Approach. *Sci. Rep.* **2019**, *9*, 20149.
(35) Kar, S.; Dutta, A.; Drew, M. G. B.; Koley, P.; Pramanik, A. Design of supramolecular β-sheet forming β-turns containing aromatic rings and non-coded α-aminoisobutyric acid and the formation of flat fibrillar structures through self-assembly. *Supramol. Chem.* **2009**, *21*, 681−690.
(36) Konar, A. D. mABA inserted supramolecular triple helix formation in the solid state in synthetic tripeptides containing β-cyanoalanine and Aib as corner residues. *CrystEngComm* **2012**, *14*, 6689−6694.
(37) Dutt, A.; Drew, M. G. B.; Pramanik, A. m-Aminobenzoic acid inserted β-turn in acyclic tripeptides: a peptidomimetic design. *Tetrahedron* **2005**, *61*, 11163−11167.
(38) Podder, D.; Sasmal, S.; Maji, K.; Haldar, D. Supramolecular tryptophan-zipper forms a tripeptide as a regular proton transporter. *CrystEngComm* **2016**, *18*, 4109−4114.
(39) Jana, P.; Maity, S.; Maity, S. K.; Haldar, D. A new peptide motif in the formation of supramolecular double helices. *Chem. Commun.* **2011**, *47*, 2092−2094.
(40) (a) Moretto, V.; Crisma, M.; Bonora, G. M.; Toniolo, C.; Balaram, H.; Balaram, P. Comparison of the Effect of Five Guest Residues on the β-Sheet Conformation of Host $(L\text{-Val})_n$ Oligopeptides. *Macromolecules* **1989**, *22*, 2939−2944.
(41) Maity, S. K.; Maity, S.; Jana, P.; Haldar, D. Supramolecular double helix from capped γ-peptide. *Chem. Commun.* **2012**, *48*, 711−713.
(42) Best, R. B.; Zhu, X.; Shim, J.; Lopes, P. E. M.; Mittal, J.; Feig, M.; Mackerell, A. D. Optimization of the Additive CHARMM All-Atom Protein Force Field Targeting Improved Sampling of the Backbone ϕ, ψ and Side-Chain χ_1 and χ_2 Dihedral Angles. *J. Chem. Theory Comput.* **2012**, *8*, 3257−3273.
(43) Bjelkmar, P.; Larsson, P.; Cuendet, M. A.; Hess, B.; Lindahl, E. Implementation of the CHARMM Force Field in GROMACS: Analysis of Protein Stability Effects from Correction Maps, Virtual Interaction Sites, and Water Models. *J. Chem. Theory Comput.* **2010**, *6*, 459−466.
(44) Jorgensen, W. L.; Chandrasekhar, J.; Madura, J. D.; Impey, R. W.; Klein, M. L. Comparison of simple potential functions for simulating liquid water. *J. Chem. Phys.* **1983**, *79*, 926−935.
(45) Bagchi, K.; Roy, S. Sensitivity of Water Dynamics to Biologically Significant Surfaces of Monomeric Insulin: Role of Topology and Electrostatic Interactions. *J. Phys. Chem. B* **2014**, *118*, 3805−3813.
(46) Haldar, D.; Maji, S. K.; Sheldrick, W. S.; Banerjee, A. First crystallographic signature of the highly ordered supramolecular helical assemblage from a tripeptide containing a non-coded amino acid. *Tetrahedron Lett.* **2002**, *43*, 2653−2656.
(47) Dutt, A.; Dutta, A.; Mondal, R.; Spencer, E. C.; Howard, J. A. K.; Pramanik, A. Studies of β-turn opening with model peptides containing non-coded α-amino isobutyric acid. *Tetrahedron* **2007**, *63*, 10282−10289.
(48) Sharma, A.; Tiwari, P.; Konar, A. D. The dominant role of side chains in supramolecular double helical organisation in synthetic tripeptides. *J. Mol. Struct.* **2018**, *1161*, 44−54.
(49) Podder, D.; Chowdhury, S. R.; Nandi, S. K.; Haldar, D. Tripeptide based super-organogelators: structure and function. *New J. Chem.* **2019**, *43*, 3743−3749.

https://doi.org/10.1021/acsomega.2c01168
ACS Omega 2022, 7, 17245−17252